

Low-Energy Test of Quantum Gravity via Angular Momentum Entanglement

Trinidad B. Lantaño,^{1,*} Luciano Petruzzello,^{1,2,3,†} Susana F. Huelga,^{1,‡} and Martin B. Plenio^{1,§}

¹*Institut für Theoretische Physik & IQST, Albert-Einstein-Allee 11, Universität Ulm, 89069 Ulm, Germany*

²*Dipartimento di Ingegneria Industriale, Università degli Studi di Salerno,*

Via Giovanni Paolo II, 132 I-84084 Fisciano (SA), Italy

³*INFN, Sezione di Napoli, Gruppo collegato di Salerno,*

Via Giovanni Paolo II, 132 I-84084 Fisciano (SA), Italy

(Dated: September 4, 2024)

Currently envisaged tests for probing the quantum nature of the gravitational interaction in the low-energy regime typically focus either on the quantized center-of-mass degrees of freedom of two spherically-symmetric test masses or on the rotational degrees of freedom of non-symmetric masses under a gravitational interaction governed by the Newtonian potential. In contrast, here we investigate the interaction between the angular momenta of spherically-symmetric test masses considering a tree-level relativistic correction related to frame-dragging that leads to an effective dipolar interaction between the angular momenta. In this approach, the mass of the probes is not directly relevant; instead, their angular momentum plays the central role. We demonstrate that, while the optimal entangling rate is achieved with a maximally delocalized initial state, significant quantum correlations can still arise between two rotating systems even when each is initialized in an eigenstate of rotation. Additionally, we examine the robustness of the generated entanglement against typical sources of noise and observe that our combination of angular momentum and spherically-symmetric test-masses mitigates the impact of many common noise sources.

Introduction – The desire to determine experimentally the character of gravity - whether it is quantum mechanical or classical in nature - remains an unmet challenge due to the extreme weakness of the gravitational interaction compared to all the other known forces. As a result, the question whether gravity and the interactions it mediates are fundamentally classical or quantum remains unanswered.

The challenge is an open one, with the earliest considerations of experimental tests dating back at least to a thought experiment proposed by Feynman during a discussion session at the 1957 *Conference on the Role of Gravitation in Physics* at Chapel Hill, North Carolina [1]. His thought experiment questioned how the gravitational field of a particle, whose center-of-mass degree of freedom is placed in a coherent superposition via a Stern-Gerlach apparatus, would act on a test mass. At the time, realizing such an experiment was entirely inconceivable, as even the control of a single quantum object such as an atom had not yet been achieved - let alone masses in the range of 10^{-14} Kg or more, where gravity becomes appreciable on realistic experimental time scales.

Recently, this question has been revisited by practitioners in the field of quantum technologies. Notably, in 2005, Lindner and Peres considered the gravitational field of a Bose-Einstein condensate in a quantum superposition and proposed probing it by scattering a particle off the condensate, which would lead to gravitationally-induced entanglement between the condensate and the particle [2]. Following these early steps, the last decade has seen an increasing number of experimental proposals aimed at elucidating the quantum nature of gravity [3–15].

When discussing this topic and its potential tests, it is essential to agree on how to define *quantum* and *classical* behavior of an interaction. To do so, it is crucial to interpret the interaction between particles as giving rise to a physical channel through which information can be exchanged and correlations

may be established. The result differs significantly depending on whether the interaction is mediated by a classical or a quantum entity. A classical interaction will henceforth be understood as any action that can be described by local quantum operations (LO) on each of the particles and an exchange of classical information (CC) between their locations - referred to collectively as LOCC [16]. A quantum mechanical interaction, however, allows for the coherent exchange of quantum states and can generate the most general quantum dynamics between the particles involved. Thus, testing the quantum nature of the object mediating the interaction involves determining the properties of the channel between the particles. If this channel can transfer an arbitrary unknown quantum state with perfect fidelity, then it is quantum; if it fails to exceed a certain fidelity, then it is a LOCC channel [17]. Another test probes whether the channel can establish entanglement between the two particles, classifying it as quantum if successful or classical if it only generates classical correlations. In the context of this work, a channel mediated by gravity is considered classical if its effect can be described by LOCC, and quantum if they cannot [3, 18, 19].

Another aspect concerns the degrees of freedom and the interaction terms considered. Current experimental proposals fall into two categories: those studying the interaction between the center-of-mass degrees of freedom of ideally spherically-symmetric particles, and those considering the rotational degrees of freedom of asymmetric objects. In both cases, the experiments proposed so far rely on the classical, non-relativistic Newtonian limit of gravity, described by the Newtonian potential between masses acting on delocalized states [20].

The experimental realization of such a test is extremely challenging. The required masses that need to be controlled and placed into well-defined quantum states need to comfortably exceed 10^{-17} Kg, which is in sharp contrast to the current

level of around 10^{-24} Kg, for which such control has been achieved [21]. Moreover, the particles must not be too close to each other, ensuring that the short-ranged Casimir-Polder forces remain negligible. This, coupled with the weakness of gravity, requires coherence times of the order of seconds. The combination of these requirements remains extremely challenging, and experimental tests of the quantum nature of gravity remain a long-term endeavor.

Mindful of these challenges, we propose an alternative platform by abandoning the Newtonian potential between center-of-mass degrees of freedom and instead considering angular momenta and the leading term of the interaction between them. This leading-order term is of relativistic origin and it is closely related to the Lense-Thirring effect of frame dragging. Adopting this setting, we then shift the problem from preparing *spatial* superpositions of center-of-mass states to preparing *angular momentum* eigenstates, which, as we will demonstrate, do not need to be in superposition to exhibit rapid entanglement generation. The high degree of symmetry of the test-masses suggests that this approach may also be less susceptible to decoherence from uncontrolled environmental degrees of freedom. In the following, we discuss our method in more detail.

The setup – Consider two spherically-symmetric microspheres A and B that are electrically neutral, free of electric dipoles, and levitated in space. These microspheres are rotating with an angular momentum L_A, L_B oriented along the z -direction, with masses M_A, M_B . The masses are held positioned along the z -axis at a distance r from each other (see Fig. 1). The rotational energy and the gravitational interaction of the angular momenta is described by the Hamiltonian

$$\hat{H} = \frac{\hbar^2 \hat{L}_A^2}{2I_A} + \frac{\hbar^2 \hat{L}_B^2}{2I_B} - \frac{GM_A M_B}{r} - \frac{G\hbar^2}{c^2 r^3} \left[\hat{\vec{L}}_A \cdot \hat{\vec{L}}_B - 3(\hat{\vec{L}}_A \cdot \vec{e}_z)(\hat{\vec{L}}_B \cdot \vec{e}_z) \right], \quad (1)$$

where I_A and I_B are the moments of inertia, \vec{L}_i denotes the angular momentum of the i -th system participating in the interaction (which is dimensionless as we already factored out an \hbar) and \vec{e}_z is the unit vector connecting the two objects [22, 23]. While other relativistic corrections exist in a fully post-Newtonian expansion of the gravitational potential [24], we limit attention to the lowest-order contributions. Equation (1) can be deduced from tree-level calculations involving canonical perturbative quantum gravity [25, 26], which, although non-renormalizable in the perturbative sense, can still yield reliable results when effective field theory methods are applied [27, 28].

For later purpose, we also introduce the angular momentum operator for the particle k as $\hat{\vec{L}}_k = \hat{L}_{kx} \vec{e}_x + \hat{L}_{ky} \vec{e}_y + \hat{L}_{kz} \vec{e}_z$, with $\hat{L}_{kx} = (\hat{L}_+ + \hat{L}_-)/2$, $\hat{L}_{ky} = (\hat{L}_+ - \hat{L}_-)/(2i)$. The angular momentum eigenstate $|l, m\rangle$ satisfies

$$\begin{aligned} \hat{L}_z |l, m\rangle &= m |l, m\rangle, \\ \hat{L}_\pm |l, m\rangle &= \sqrt{l(l+1) - m(m \pm 1)} |l, m \pm 1\rangle. \end{aligned} \quad (2)$$

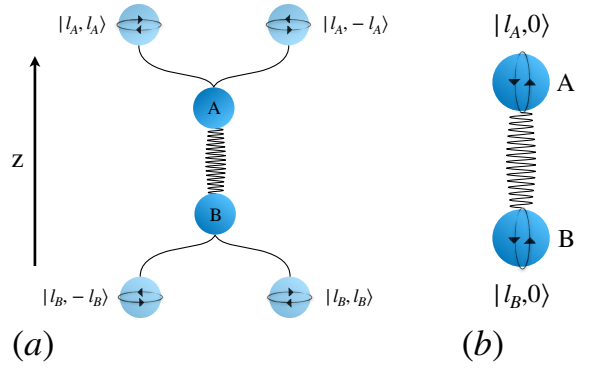


Figure 1. Pictorial representation of the initial state preparation. With reference to Eq. (3), we consider then scenario with: (a) $m_i = 0$ and (b) $m_i = l_i$ where $i = \{A, B\}$.

Initial state and entanglement build-up – We assume two levitated microspheres prepared in the product state

$$\begin{aligned} |\psi_{AB}\rangle &= \mathcal{N} (|l_A, m_A\rangle + |l_A, -m_A\rangle) \\ &\otimes (|l_B, m_B\rangle + |l_B, -m_B\rangle), \end{aligned} \quad (3)$$

where \mathcal{N} is the normalization factor. Since the operator \hat{L}^2 commutes with all its components, in the interaction picture with respect to the kinetic part the Hamiltonian (1) reads

$$\hat{H}_I = -\frac{\alpha\hbar}{2} \left(\hat{L}_{A+} \hat{L}_{B-} + \hat{L}_{A-} \hat{L}_{B+} - 4\hat{L}_{Az} \hat{L}_{Bz} \right), \quad (4)$$

where $\alpha := G\hbar/(c^2 r^3)$. For a compact notation, we henceforth write $|l_i, m_i\rangle := |m\rangle_i$ and find the state at time t to be

$$\begin{aligned} |\psi_{AB}(t)\rangle &= \mathcal{N} e^{\frac{i\alpha t}{2} (\hat{L}_{A+} \hat{L}_{B-} + \hat{L}_{A-} \hat{L}_{B+} - 4\hat{L}_{Az} \hat{L}_{Bz})} \\ &\cdot (|m\rangle_A + |-m\rangle_A) (|m\rangle_B + |-m\rangle_B). \end{aligned} \quad (5)$$

Since the state is pure, we compute the amount of entanglement via the Von Neumann entropy $\mathcal{S}(\rho) := -\sum_i \eta_i \log_2 \eta_i$, where ρ is the density matrix of a bipartite system AB and η_i are the eigenvalues of the reduced density matrix of one of the subsystems. Expanding the exponential operator in Eq. (5) up to second order yields

$$|\psi_{AB}(t)\rangle = \left(\mathbb{1} + \frac{i\alpha t}{2} \hat{O}_{AB} - \frac{\alpha^2 t^2}{8} \hat{O}_{AB} \hat{O}_{AB} \right) |\psi_{AB}(0)\rangle, \quad (6)$$

where $\hat{O}_{AB} := \hat{L}_{A+} \hat{L}_{B-} + \hat{L}_{A-} \hat{L}_{B+} - 4\hat{L}_{Az} \hat{L}_{Bz}$. Let us define the couplings $\kappa(m, t) := \alpha t m^2 / 2$, where $-l \leq m \leq l$ and $g := \kappa(l, t) = \alpha t l^2 / 2$. By keeping only contributions up to κ^2 and g^2 , we obtain

$$\begin{aligned} \mathcal{S}(\rho_{AB}) &= \\ &= (2g^2 - 4g\kappa + 18\kappa^2 - 1) \log_2 (-2g^2 + 4g\kappa - 18\kappa^2 + 1) \\ &\quad - 4(g - \kappa)^2 \log_2 (g - \kappa) - 32\kappa^2 \log_2 (4\kappa). \end{aligned} \quad (7)$$

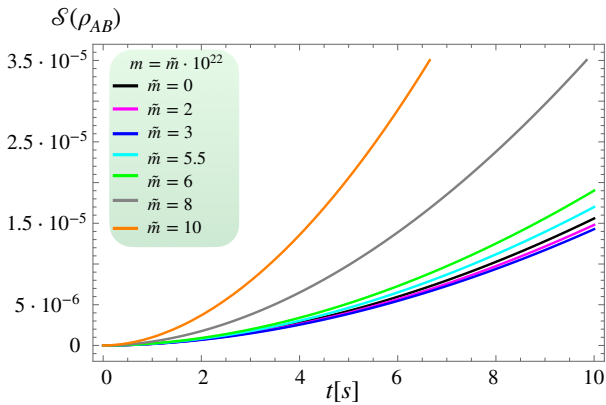


Figure 2. Time evolution of the von Neumann entropy as given by Eq. (7) for $l = 10^{23}$. Each curve corresponds to a different m quantum number as defined in Eq. (5). While the largest entangling rate is achieved for $m = l$, even the more easily prepared $m = 0$ configuration yields significant rates.

Higher-order contributions in κ and g are negligible in the scenario typical for the remainder of this work: We consider two identical silica (SiO_2) micro-spheres with mass density $\rho = 2200 \text{ kg/m}^3$, radius $R = 50 \text{ }\mu\text{m}$, a center-of-mass separation of $r = 4R$ and rotation frequencies $\omega = 10^7 \text{ Hz}$. This yields $\alpha t \approx 10^{-50}t$, where t is the evolution time. The total angular momentum is $L_A = L_B = L = 8\pi\omega\rho R^5/15 \approx 1.15 \cdot 10^{-11} \text{ J}\cdot\text{s}$, which gives a quantum number $l_A = l_B = l = L/\hbar \approx 10^{23}$. Since $l \gg 1$, we can write the action of the ladder operators as $\hat{L}_+ |0\rangle = \sqrt{l(l+1)} |1\rangle \approx l |1\rangle$, $\hat{L}_- |0\rangle = \sqrt{l(l+1)} |-1\rangle \approx l |-1\rangle$. In this case, we only obtain terms proportional to $\kappa \leq g = \alpha t l^2 / 2 \approx 6 \cdot 10^{-5}t$, and for reasonable duration of the experiment our approximation is satisfied.

Importantly, we observe that, although $m = l$ provides the fastest entanglement growth rate, even the eigenstate of angular momentum with $m = 0$ yields significant entangling rates, exceeding those with m -quantum numbers of up to $m \approx 0.95 l$. While the rates are lower, the gain in the facility of producing the initial state for $m = 0$ may well outweigh the moderate reduction in the entangling rate.

Decoherence – The scenario described so far represents an idealization in which the system is assumed to be completely isolated from its environment. However, in reality, various interactions with the environment lead to decoherence. Nevertheless, it is important to note that, in our set-up, the choice of angular momentum as the degree of freedom and the assumption of almost perfect spherical symmetry in the test masses reduce the impact of many noise sources that plague experiments probing the Newtonian potential via spatial delocalization or rotational degree of freedom for asymmetric particles. Indeed, the almost perfect spherical symmetry of the mass distribution entails that the impact of the Casimir-Polder forces is reduced significantly. Therefore, the upcoming discussion will focus on evaluating the implications of three major sources of decoherence in the gravitational channel: (i)

magnetic dipole-dipole interaction, (ii) collisions with surrounding particles, and (iii) black-body radiation. Additionally, we will explore the implications of rotating the microspheres up to 10^7 Hz .

While many materials may be suitable for the type of experiment we propose here, microspheres of amorphous silica are routinely levitated and have already been made to rotate at angular frequencies of up to 6 GHz for particles of 190 nm diameter [29]. Therefore, in the following we will base our estimates for the experimental requirements on this material.

- *Magnetic dipole-dipole interaction* – Amorphous silica is mainly made up by neutral and spinless nuclei, the only source of a non-vanishing spin coming from the spin-1/2 of ^{29}Si , while the most abundant isotope of silicon is ^{28}Si . Isotope separation can reduce the ^{29}Si content to the ppm level [30]. This would imply around $n \simeq 10^9$ nuclear spins in a silica microsphere of radius $50 \mu\text{m}$.

As a result, the interaction energy associated with the magnetic dipole-dipole interaction would be $V_M \simeq 10^{-28} p^2 \text{ J}$, with p the polarization. If (as before) angular momentum is of the order of $L \simeq 10^{-11} \text{ J}\cdot\text{s}$, then the gravitational potential in eq. (1) is equal to $V_G \simeq 10^{-38} \text{ J}$, implying that

$$\frac{V_M}{V_G} \simeq p^2 10^{10}. \quad (8)$$

In thermal equilibrium at $T = 1 \text{ K}$ and with an applied magnetic field of $B = 1 \text{ T}$, the thermal polarization of the ^{29}Si is $p \simeq 10^{-5}$. If required (e.g., for lower temperatures where the thermal polarization p increases or accounting for very small impurity concentrations bearing electron spins), a Faraday shield may be inserted between the two microspheres to further suppress the electromagnetic interaction. Thus, gravity can safely be assumed to be the main source of entanglement between the two test objects.

- *Collisions* – To determine the rate of events, r , of collisions with air dust, imagine the microsphere moving at the typical speed of an air particle at a temperature $T = 1 \text{ K}$, that is, $v_{\text{air}} \approx 30 \text{ m/s}$, while the surrounding gas remains stationary. The volume of the resulting cylinder over time t is calculated using $V = \pi R^2 v_{\text{air}} t$. Given a low pressure $P = 10^{-15} \text{ Pa}$, we can derive a particle density of $\rho_{\text{air}} = 10^{-18} \text{ kg/m}^3$. Considering the mass of an air particle as $m_{\text{air}} = 10^{-26} \text{ kg}$, we approximate the collision rate as $r = V \rho_{\text{air}} / (m_{\text{air}} t) \approx 10$ collisions per second.

To streamline the following analysis, we focus on a single collision and require that such an event is able to change only the m number by an unknown amount q up to a maximum $n < l$ while leaving the l quantum number untouched. If the probability of k of such events happening during a time interval t is described by the Poisson distribution $P(k; t) = (rt)^k e^{-rt} / k!$, where r is the average rate of events, the state

will be given by (up to a normalization factor)

$$\rho_{AB} = P(0; t) \rho_0 + P(1; t) \sum_{q=1}^n \rho_{A+}^q + \rho_{A-}^q + \rho_{B+}^q + \rho_{B-}^q, \quad (9)$$

where

$$\begin{aligned} \rho_0(t) &= |\psi_{AB}(t)\rangle\langle\psi_{AB}(t)|, \\ \rho_{A\pm}^q(t) &= (\hat{L}_{A\pm})^q |\psi_{AB}(t)\rangle\langle\psi_{AB}(t)| (\hat{L}_{A\mp})^q, \end{aligned} \quad (10)$$

with $|\psi_{AB}(t)\rangle$ given by Eq. (6) and where we have implicitly assumed q to be uniformly distributed.

Since (9) is a mixed state, we use the Logarithmic Negativity $E_N(\rho)$ [31], defined as $E_N(\rho) = \log_2 \|\rho^{\Gamma A}\|_1$, where $\|\cdot\|_1$ denotes the trace norm and $\rho^{\Gamma A}$ is the partial transpose of ρ with respect to system A. We obtain numerical results for $E_N(\rho_{AB}(t))$ in two cases, namely when the state is initially prepared as in Eq. (3), either with $m = 0$ or $m = l$. In both cases, we assume the same total angular momentum $l = 10^{23}$ (see Fig. (3)). We observe that, even for one collision and in

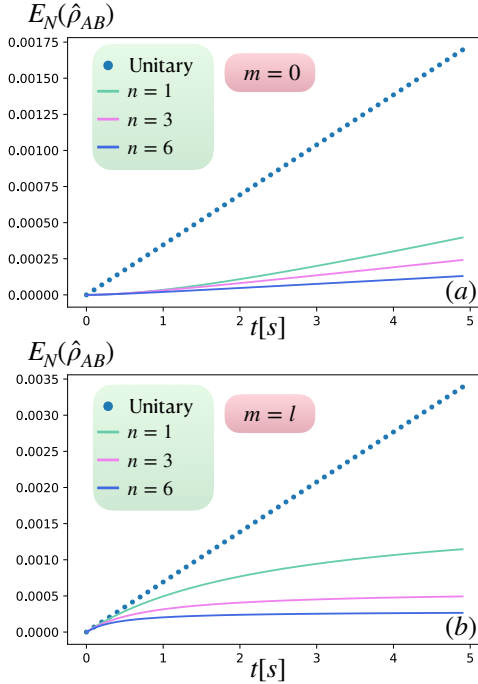


Figure 3. Logarithmic negativity of state (9) as a function of time considering $n = \{1, 3, 6\}$. We study the decoherence of the state given by Eq. (5) in two cases: (a) $m = 0$ and (b) $m = l$.

the optimistic assumption of no change to the l quantum number, the entanglement drops dramatically, which leads us to conclude that, in order to preserve and detect entanglement, the safest scenario needs to ensure that the probability for a collision is well below unity.

• **Black-body radiation** – Apart from collisions with particles from the background gas, also the emission or absorption

of a photon has the potential to change the angular momentum quantum numbers l and m . Hence, the impact of black-body radiation on the evolution of Eq. (5) needs to be analyzed carefully.

We describe the absorption and emission of thermal photons in an open quantum system approach. While this method aligns conceptually with [32, 33], it is important to note that our procedure focuses on angular momentum degrees of freedom rather than orientational ones (*i.e.*, Euler angles).

Regarding the system density matrix $\hat{\rho}_S$ defined on the Hilbert space $\mathcal{H}_A \otimes \mathcal{H}_B$, see Appendix I for a detailed derivation of a quantum master equation which describes the joint evolution of spheres A and B as they undergo the gravitational interaction (1) along with a dissipative evolution caused by a thermal bath. Assuming that the characteristic wavelength of the photons is larger than the separation between the masses, the equation reads

$$\begin{aligned} \frac{d}{dt} \hat{\rho}_S(t) &= -\frac{i}{\hbar} [\hat{H}_I^{AB}, \hat{\rho}_S(t)] \\ &+ \sum_{l \geq 0} \sum_p \left[\hat{C}_{l,p} \hat{\rho}_S(t) \hat{C}_{l,p}^\dagger - \frac{1}{2} \{ \hat{C}_{l,p}^\dagger \hat{C}_{l,p}, \hat{\rho}_S(t) \} \right] \\ &+ \sum_{l \geq 0} \sum_p \left[\hat{F}_{l,p} \hat{\rho}_S(t) \hat{F}_{l,p}^\dagger - \frac{1}{2} \{ \hat{F}_{l,p}^\dagger \hat{F}_{l,p}, \hat{\rho}_S(t) \} \right], \end{aligned} \quad (11)$$

where $p = \{1, 2, 3\}$, $\{\cdot, \cdot\}$ denotes the anticommutator, $\hat{C}_{l,p} := \sqrt{\chi_l} \hat{A}_p^{AB}(\Delta_l)$ and $\hat{F}_{l,p} := \sqrt{\gamma_l} \hat{A}_p^{AB\dagger}(\Delta_l)$ are collapse operators, with $\hat{A}^{AB} = \sum_i \hat{A}_i \vec{v}_i \otimes \mathbb{1} + \mathbb{1} \otimes \sum_i \hat{A}_i \vec{v}_i$ and \hat{A}_i given by Eqs. (51-53) in the Appendix. The rates are

$$\begin{aligned} \chi_l &:= \frac{\Delta_l^3 \hbar^2}{6c^3 I^3 \epsilon_0} (1 + N(\Delta_l)) d_{\text{eff}}^2, \\ \gamma_l &:= \frac{\Delta_l^3 \hbar^2}{6c^3 I^3 \epsilon_0} N(\Delta_l) d_{\text{eff}}^2. \end{aligned} \quad (12)$$

Here, $\Delta_l := 2(l+1)$ with the moment of inertia I of one microsphere, $N(\cdot)$ the mean occupation number given in Eq. (42) of the Appendix and ϵ_0 the permittivity of free space.

To determine γ_l and χ_l we need the effective dipole moment d_{eff} . As the amorphous silica microspheres are dielectric, we assume a polarization $P = \epsilon_0(\epsilon_r - 1)E(T, \lambda)$, where ϵ_r is the relative permittivity of the material and $E(T, \lambda)$ is the electric field amplitude of the thermal radiation at temperature T and wavelength λ . On the other hand, the polarization can be seen as the density of dipoles in a certain volume V , that is, $P = d_{\text{eff}}/V$. Therefore, an estimation of the effective dipole moment of each sphere is given by $d_{\text{eff}} = V(\epsilon_r - 1)\sqrt{2\epsilon_0}u(T, \lambda)$, where we have introduced the energy density $u(T, \lambda) = E^2(T, \lambda)\epsilon_0/2$. Using Planck's law for $u(T, \lambda)$ and Wien's law to replace the wavelength by the one that gives the maximum energy density $\lambda_{\text{peak}} = b/T$ where $b \approx 2.8 \cdot 10^{-3} \text{ m} \cdot \text{K}$, we have

$$d_{\text{eff}} = \sqrt{\frac{32\pi^2 V^2 (\epsilon_r - 1)^2 c \hbar \epsilon_0 T^5}{b^5 \left(e^{\frac{2\pi \hbar c}{b k_B}} - 1 \right)}}. \quad (13)$$

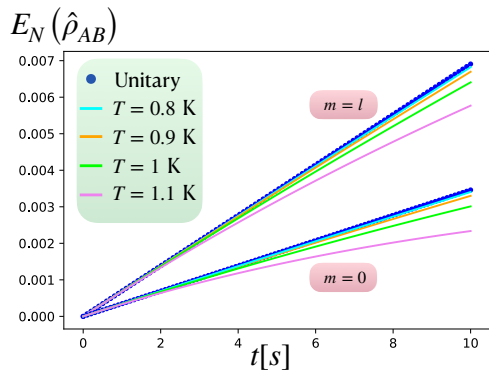


Figure 4. Logarithmic negativity of the state given by Eq. (11) as a function of time. We study the black-body decoherence of state (5) in two cases: (lower) $m = 0$ and (upper) $m = l$.

With the knowledge of d_{eff} and the physical details of the microspheres introduced before, we have that, when the state is prepared with $m = l$ in Eq. (3) and evolved according to Eq. (11) at $T = 0.6$ K, the decoherence rate is $\gamma_l \approx 2 \cdot 10^{-4} \text{ s}^{-1}$, while the variation of logarithmic negativity under unitary evolution after $t = 10$ s is $\dot{E}_N := \Delta E_N(\hat{\rho}_S)/\Delta t \approx 7 \cdot 10^{-4} \text{ s}^{-1}$. This indicates that, at $T = 0.6$ K, the black-body radiation decoherence will not dominate over entanglement generation. However, a small increase in temperature, e.g., $T=0.8$ K, already gives $\gamma_l \approx 0.001 \text{ s}^{-1}$, which surpasses the entanglement rate. Remarkably, the fact that γ_l surpasses \dot{E}_N does not result in a complete suppression of entanglement build-up. Indeed, Fig. (4) shows that, for $T=0.8$ K, the curve deviates slightly from the unitary evolution, and even for $T = 1.1$ K, where $\gamma_l \approx 0.008 \text{ s}^{-1}$ – one order of magnitude larger than \dot{E}_N – we do not observe a significant drop in the entanglement rate.

Given that we assume both particles interact with the same bath (as discussed at the beginning of the Appendix), one might wonder whether any entanglement arises due to the radiation field. To explore this possibility, we simulated Eq. (11) with $\dot{H}_I^{AB} = 0$ and observed that the negativity remained zero over the time scales considered.

• *Laser heating* – As a final observation, one must account for the fact that, in order to generate high-frequency rotations, lasers must be employed [29]. However, the use of lasers is responsible for the heating of the spheres, which can thus quickly approach an undesired value of the temperature. To estimate the increase in T , one can rely on the following equation [34, 35]:

$$\int_{T_i}^{T_f} dT c_M(T) = \frac{4\omega_f \lambda^2}{a R \rho} \text{Im} \left[\frac{\varepsilon - 1}{\varepsilon + 2} \right], \quad (14)$$

where T_i (T_f) is the initial (final) temperature before (after) the application of the laser of wavelength λ which brings the frequency rotation of a sphere with radius R , density ρ , specific heat capacity $c_M(T)$ and refractive index n (such that $\varepsilon = n^2$) up to ω_f , with $a = 8.15 \cdot 10^{-11} \text{ m}^4/(\text{W}\cdot\text{s}^2)$.

Since we are considering low temperatures, the Debye model [36] is a good approximation for the behavior of c_M as a function of T , that is, $c_M(T) = \beta T^3$, with $\beta \approx 3 \cdot 10^{-4} \text{ J}/(\text{Kg}\cdot\text{K}^4)$ for the amorphous silica [37]. With an initial temperature of 1 K, a desired rotation frequency of 10^7 Hz, a range of wavelength for the laser slightly outside the visible spectrum (i.e., $\lambda = 300$ nm) and a refractive index of $n = 1.47 + i(0.01\lambda/(4\pi))$ [35, 37], it is straightforward to prove that $T_f \approx 1.13$ K, thus implying that, according to the previous analysis of radiative decoherence, the disturbance due to the use of the laser is not substantial.

Final remarks – In this Letter, we have shifted the paradigm of gravitationally-induced entanglement tests by introducing a new protocol based on the post-Newtonian interaction (1), which is capable of entangling the angular momentum degrees of freedom rather than the positional ones. In so doing, we have shown how, under suitable conditions and in spite of decoherence channels, the entanglement generation is sufficiently relevant even when the initial states of the involved systems are not in a quantum superposition.

On a final note, it is worth emphasizing that the idea of employing angular momentum for the gravitational generation of entanglement has been suggested also in Ref. [38]. However, in the said work the main purpose is to exploit high rotational frequencies to enhance the energy of the test masses and invoke the mass-energy equivalence principle to boost the entanglement growth by still relying on positional degrees of freedom.

Acknowledgements – This work was supported by the ERC Synergy Grant HyperQ (Grant No. 856432), the EU project QuMicro (grant no. 01046911) and the DFG via QuantERA project LemaQume (Grant No. 500314265). We acknowledge discussions with Julen Pedernales at early stages of the project.

I. APPENDIX: MICROSCOPIC DERIVATION OF THE MASTER EQUATION

In order to derive a master equation that captures the effect of black-body radiation on our proposed experiment, we consider two bound quantum systems (atoms or molecules) that interact through the potential Eq. (4) while immersed in a quantized radiation field [39]. Subsequently, we extend our analysis to a mesoscopic system, *i.e.*, the SiO₂ microspheres.

The starting point is the total Hamiltonian for the closed system, which includes the systems A and B as well as the environment, modeled as a thermal reservoir of bosonic modes

$$\hat{H} = \hat{H}_0 + \hat{H}_E + \hat{H}_I, \quad (15)$$

where

$$\hat{H}_0 = \hat{h}_0 \otimes \mathbb{1} + \mathbb{1} \otimes \hat{h}_0, \quad \hat{h}_0 := \frac{\hbar^2 \hat{L}^2}{2I}, \quad (16)$$

$$\hat{H}_E = \sum_{\mathbf{k}} \hbar \omega_{\mathbf{k}} \hat{a}_{\mathbf{k}}^\dagger \hat{a}_{\mathbf{k}}, \quad (17)$$

$$\hat{H}_I = \hat{H}_I^{AB} + \hat{H}_I^{ABE}, \quad (18)$$

where \hat{L}^2 is a one-particle angular momentum operator, I is the inertial moment of each sphere, $\omega_{\mathbf{k}} = |\vec{k}|c$ and the sum over \mathbf{k} also includes the polarizations of the electromagnetic field. Note that \hat{H}_0 acts on the subspace of the two particles AB . If we consider the center of mass of spheres A and B to be located in $\vec{r}^A = \vec{0}$ and $\vec{r}^B = \vec{r}_0$ and denote their dipole moments as \hat{D}^A and \hat{D}^B , respectively, we have

$$\hat{H}_I^{AB} := -\frac{\alpha \hbar}{2} \left(\hat{L}_{A+} \hat{L}_{B-} + \hat{L}_{A-} \hat{L}_{B+} - 4\hat{L}_{Az} \hat{L}_{Bz} \right), \quad (19)$$

$$\begin{aligned} \hat{H}_I^{ABE} &= -\left(\hat{D}^A \cdot \hat{E}(\vec{0}) + \hat{D}^B \cdot \hat{E}(\vec{r}_0) \right) = -\left(\hat{D}^A \cdot \hat{E} + \hat{D}^B \cdot \hat{E} e^{i\vec{k} \cdot \vec{r}_0} \right) \\ &\approx -\left(\hat{D}^A + \hat{D}^B \right) \cdot \hat{E}, \end{aligned} \quad (20)$$

where the operators labeled with $A(B)$ are understood to act only on the subspace of the particle $A(B)$. Note that the last approximation is only valid as long as $\vec{k} \cdot \vec{r}_0 \ll 1$, meaning that the electric field wavelength is much larger than the separation between the spheres. In our case, we consider a center of mass separation of $|\vec{r}_0| = 2 \cdot 10^{-4}$ m and a characteristic wavelength of $\lambda = hc/k_B T \simeq 10^{-2}/T$. Therefore, at $T = 1$ K or below, the conditions for the approximation (20) are fulfilled.

On the other hand, the electric field can be decomposed in the second quantization scheme as

$$\hat{E} = i \sum_{\mathbf{k}} \sqrt{\frac{2\pi \hbar \omega_{\mathbf{k}}}{V \epsilon_0}} \vec{e}_{\mathbf{k}} \left(\hat{a}_{\mathbf{k}} - \hat{a}_{\mathbf{k}}^\dagger \right), \quad (21)$$

with $\vec{e}_{\mathbf{k}}$ being the polarization vector, V the volume of the box used to write the discretized expansion of the field and ϵ_0 the permittivity of free space.

Now, the Hamiltonian employed so far is the result of two underlying assumptions: i) the interaction between the thermal bath and each microsphere is treated as if each mesoscopic object is a big atom with appropriate angular momentum eigenstates and a suitably determined effective dipole strength; ii) both microspheres interact with the same thermal bath. The first requirement is a simplification that allows us to write the dipole moment of each microsphere as

$$\hat{D}^A = \hat{d} \otimes \mathbb{1}, \quad \hat{D}^B = \mathbb{1} \otimes \hat{d}, \quad (22)$$

where $\hat{d} = q_{\text{eff}} \hat{r}$, q_{eff} is an effective charge to be estimated and \hat{r} the position operator, whilst the second requirement is reflected in the approximation (20). Next, moving to the interaction picture with respect to \hat{H}_0 and \hat{H}_E , we have

$$\hat{H}_I(t) = \hat{H}_I^{AB} + \hat{H}_I^{ABE}(t). \quad (23)$$

The equation for the reduced density matrix of the system AB then becomes

$$\frac{d}{dt} \hat{\rho}_S(t) = -\frac{i}{\hbar} \left[\hat{H}_I^{AB}, \hat{\rho}_S(t) \right] - \frac{i}{\hbar} \text{Tr}_E \left[\hat{H}_I^{ABE}(t), \hat{\rho}(t) \right], \quad (24)$$

where $\hat{\rho}_S := \text{Tr}_E \hat{\rho}$ and $\hat{\rho}$ is the density matrix of the full system ABE . From Eq. (24), we can already verify that the unitary part of the evolution only depends on the gravitational interaction between A and B . Bearing this in mind, let us insert the integral form of $\hat{\rho}(t)$, given by

$$\hat{\rho}(t) = \hat{\rho}(0) - \frac{i}{\hbar} \int_0^t ds \left[\hat{H}_I(s), \hat{\rho}(s) \right], \quad (25)$$

into the second term of the r.h.s. in Eq. (24), thus obtaining

$$-\frac{i}{\hbar} \text{Tr}_E \left[\hat{H}_I^{ABE}(t), \hat{\rho}(t) \right] = -\frac{1}{\hbar^2} \int_0^t ds \text{Tr}_E \left[\hat{H}_I^{ABE}(t), \left[\hat{H}_I(s), \hat{\rho}(s) \right] \right] = -\frac{1}{\hbar^2} \int_0^t ds \text{Tr}_E \left[\hat{H}_I^{ABE}(t), \left[\hat{H}_I(s), \hat{\rho}_S(t) \otimes \hat{\rho}_E \right] \right], \quad (26)$$

where we assume $\text{Tr}_E \left[\hat{H}_I^{ABE}(t), \hat{\rho}(0) \right] = 0$ and perform the Born approximation, *i.e.*, $\hat{\rho}(s) \approx \hat{\rho}_S(s) \otimes \hat{\rho}_E$ followed by the Markov approximation, according to which we replace $\hat{\rho}(s)$ by $\hat{\rho}(t)$ in order to have an equation local in time.

To achieve a Markovian master equation, we can substitute the variable s with $t - s$ and push the extremal of the integral to infinity provided that the integrand goes to zero sufficiently fast [39]. In light of this, Eq. (24) becomes

$$\frac{d}{dt} \hat{\rho}_S(t) = -\frac{i}{\hbar} \left[\hat{H}_I^{AB}, \hat{\rho}_S(t) \right] - \frac{1}{\hbar^2} \int_0^\infty ds \text{Tr}_E \left[\hat{H}_I^{ABE}(t), \left[\hat{H}_I(t-s), \hat{\rho}_S(t) \otimes \hat{\rho}_E \right] \right]. \quad (27)$$

Assuming that $\hat{\rho}_E$ is given by a thermal state, that is

$$\hat{\rho}_E = \frac{\exp(-\beta \hat{H}_E)}{\text{Tr}_E \exp(-\beta \hat{H}_E)}, \quad \beta = \frac{1}{k_B T}, \quad (28)$$

it is straightforward to check that

$$\langle \hat{E} \rangle = \text{Tr}_E \left(\hat{E} \hat{\rho}_E \right) = i \sum_{\mathbf{k}} \sqrt{\frac{2\pi\hbar\omega_{\mathbf{k}}}{V\epsilon_0}} \vec{e}_{\mathbf{k}} \left(\langle \hat{a}_{\mathbf{k}} \rangle - \langle \hat{a}_{\mathbf{k}}^\dagger \rangle \right) = 0, \quad (29)$$

thereby simplifying Eq. (27) to

$$\frac{d}{dt} \hat{\rho}_S(t) = -\frac{i}{\hbar} \left[\hat{H}_I^{AB}, \hat{\rho}_S(t) \right] - \frac{1}{\hbar^2} \int_0^\infty ds \text{Tr}_E \left[\hat{H}_I^{ABE}(t), \left[\hat{H}_I^{ABE}(t-s), \hat{\rho}_S(t) \otimes \hat{\rho}_E \right] \right], \quad (30)$$

since only quadratic terms in the environmental operators are non-vanishing.

In order to cast Eq. (30) in a Lindblad form, the recipe is to re-write the interaction Hamiltonian $\hat{H}_I^{ABE}(t)$ in terms of eigenoperators of the system \hat{H}_0 [39]. First, note that the angular momentum states $|l, m\rangle$ are eigenkets of \hat{h}_0 with eigenvalues $E_l = \hbar^2 l(l+1)/(2I)$. For simplicity, we are going to consider the same angular momentum for both spheres, meaning $l_A = l_B = l$. At this point, we define the one particle operator

$$\hat{A}(\Delta) := \sum_{\substack{m, m' \\ l, l' \text{ s.t. } E_{l'} - E_l = \frac{\hbar^2}{2I} \Delta}} |l, m\rangle \langle l, m| \hat{d} |l', m'\rangle \langle l', m'|, \quad (31)$$

with $-l \leq m \leq l$, $-l' \leq m' \leq l'$ and where Δ is a fixed value. Note that Δ can only be an even integer. Now, for both spheres we introduce the quantity

$$\hat{A}^{AB} := \hat{A} \otimes \mathbf{1} + \mathbf{1} \otimes \hat{A} \quad (32)$$

$$= \sum_{\substack{m, m' \\ l, l' \text{ s.t. } E_{l'} - E_l = \frac{\hbar^2}{2I} \Delta}} \langle l, m | \hat{d} | l', m' \rangle \left[|l, m\rangle \langle l', m'| \otimes \mathbf{1} + \mathbf{1} \otimes |l, m\rangle \langle l', m'| \right], \quad (33)$$

which is an eigenoperator of the system as

$$\left[\hat{h}_0, \hat{A}(\Delta) \right] = -\frac{\hbar^2}{2I} \Delta \hat{A}(\Delta), \quad \left[\hat{h}_0, \hat{A}^\dagger(\Delta) \right] = \frac{\hbar^2}{2I} \Delta \hat{A}^\dagger(\Delta). \quad (34)$$

One can then see that, when switching to the interaction picture, \hat{A}^{AB} only acquires a time-dependent phase

$$e^{\frac{i\hat{H}_0 t}{\hbar}} \hat{A}^{AB}(\Delta) e^{-\frac{i\hat{H}_0 t}{\hbar}} = e^{-\frac{it\hbar\Delta}{2I}} \hat{A}^{AB}(\Delta), \quad e^{\frac{i\hat{H}_0 t}{\hbar}} \hat{A}^{AB\dagger}(\Delta) e^{-\frac{i\hat{H}_0 t}{\hbar}} = e^{\frac{it\hbar\Delta}{2I}} \hat{A}^{AB\dagger}(\Delta). \quad (35)$$

Furthermore, by using the completeness relation for angular momentum states, one can sum over Δ in Eq. (31) to obtain

$$\sum_{\Delta \in 2\mathbb{Z}} \hat{A}(\Delta) = \hat{d}, \quad (36)$$

where $2\mathbb{Z}$ denotes the set of even integers. In the interaction picture, this entails

$$\hat{D}^{AB}(t) = \sum_{\Delta \in 2\mathbb{Z}} e^{-\frac{i\hbar t\Delta}{2I}} \hat{A}^{AB}(\Delta) = \sum_{\Delta \in 2\mathbb{Z}} e^{\frac{i\hbar t\Delta}{2I}} \hat{A}^{AB\dagger}(\Delta), \quad (37)$$

where we used $\hat{A}^{AB\dagger}(\Delta) = \hat{A}^{AB}(-\Delta)$.

We now have all the tools to convert Eq. (30) into a Lindblad-type master equation. By inserting the dipole moment (37) into Eq. (30) and working out the nested commutator, we arrive at

$$\frac{d}{dt} \hat{\rho}_S(t) = -\frac{i}{\hbar} \left[\hat{H}_I^{AB}, \hat{\rho}_S(t) \right] + \sum_{\substack{\Delta, \Delta' \\ p, q=1,2,3}} e^{\frac{i\hbar(\Delta' - \Delta)t}{2I}} \Gamma_{pq}(\Delta) \left[\hat{A}_q^{AB}(\Delta) \hat{\rho}_S(t) \hat{A}_p^{AB\dagger}(\Delta') - \hat{A}_p^{AB\dagger}(\Delta') \hat{A}_q^{AB}(\Delta) \hat{\rho}_S(t) \right] + \text{h.c.}, \quad (38)$$

where we implicitly assume that the sum is carried over the even integers, \hat{A}_p^{AB} denotes the p -th component of \hat{A}^{AB} in some orthonormal basis $\{\vec{v}_1, \vec{v}_2, \vec{v}_3\}$ and

$$\Gamma_{pq}(\Delta) = \int_0^\infty ds e^{\frac{i\hbar s\Delta}{2I}} \left\langle \hat{E}_p(t) \hat{E}_q(t-s) \right\rangle. \quad (39)$$

Noting that on a thermal state $\left\langle \hat{E}_p(t) \hat{E}_q(t-s) \right\rangle = \left\langle \hat{E}_p(s) \hat{E}_q(0) \right\rangle$, we can perform the rotating wave approximation in Eq. (38), where we only consider terms for which $\Delta' = \Delta$. This holds true because the phase factors in Eq. (38) oscillate very rapidly in time intervals where the operator $\hat{\rho}_S(t)$ changes appreciably. Bearing this in mind, we write

$$\frac{d}{dt} \hat{\rho}_S(t) = -\frac{i}{\hbar} \left[\hat{H}_I^{AB}, \hat{\rho}_S(t) \right] + \sum_{\substack{\Delta \\ p, q=1,2,3}} \Gamma_{pq}(\Delta) \left[\hat{A}_q^{AB}(\Delta) \hat{\rho}_S(t) \hat{A}_p^{AB\dagger}(\Delta) - \hat{A}_p^{AB\dagger}(\Delta) \hat{A}_q^{AB}(\Delta) \hat{\rho}_S(t) \right] + \text{h.c.}. \quad (40)$$

At this stage, there is no substantial difference with respect to the standard treatment of open quantum systems when it comes to evaluate the factor $\Gamma_{pq}(\Delta)$. In particular, as we chose a thermal reservoir, the correlation functions of the electric field can be easily computed [39, 40] and, if we neglect the contributions associated to the renormalization of the system Hamiltonian (namely, Lamb and Stark shift terms), we arrive at the expression

$$\begin{aligned} \frac{d}{dt} \hat{\rho}_S(t) = & -\frac{i}{\hbar} \left[\hat{H}_I^{AB}, \hat{\rho}_S(t) \right] \\ & + \sum_{\Delta > 0} \frac{\Delta^3 \hbar^2}{6c^3 I^3 \epsilon_0} (1 + N(\Delta)) \left[\hat{A}^{AB}(\Delta) \cdot \hat{\rho}_S(t) \hat{A}^{AB\dagger}(\Delta) - \frac{1}{2} \left\{ \hat{A}^{AB\dagger}(\Delta) \cdot \hat{A}^{AB}(\Delta), \hat{\rho}_S(t) \right\} \right] \\ & + \sum_{\Delta > 0} \frac{\Delta^3 \hbar^2}{6c^3 I^3 \epsilon_0} N(\Delta) \left[\hat{A}^{AB\dagger}(\Delta) \cdot \hat{\rho}_S(t) \hat{A}^{AB}(\Delta) - \frac{1}{2} \left\{ \hat{A}^{AB}(\Delta) \cdot \hat{A}^{AB\dagger}(\Delta), \hat{\rho}_S(t) \right\} \right], \end{aligned} \quad (41)$$

where

$$N(\Delta) = \frac{1}{\exp\left(\frac{\beta \hbar^2 \Delta}{2I}\right) - 1}, \quad (42)$$

is the average number of photons with energy $\hbar^2 \Delta / 2I$ as given by the Planck distribution. Although this is the final expression for our master equation, there is still one last task to complete. As a matter of fact, we have not yet provided the matrix element

of the dipole moment in the angular momentum representation $\langle l, m | \hat{d} | l', m' \rangle$, which turns out to be crucial to compute the jump operators (31). In spherical coordinates, we have

$$\langle l, m | \hat{d} | l', m' \rangle = q_{\text{eff}} R \left(\langle l, m | \sin \hat{\theta} \cos \hat{\varphi} | l', m' \rangle \vec{e}_x + \langle l, m | \sin \hat{\theta} \sin \hat{\varphi} | l', m' \rangle \vec{e}_y + \langle l, m | \cos \hat{\theta} | l', m' \rangle \vec{e}_z \right), \quad (43)$$

where R is the radius of both spheres A and B . In general, when computing the expectation value of a function of the spherical angles $f(\hat{\theta}, \hat{\varphi})$ on angular momentum eigenstates, it is convenient to introduce the direction eigenkets $|\vec{n}\rangle$, which are eigenvectors of the angles $\hat{\theta}$ and $\hat{\varphi}$ with eigenvalues θ and φ , respectively. Furthermore, these states fulfill the completeness relation [41]

$$\int d\Omega |\vec{n}\rangle \langle \vec{n}| = \int_0^{2\pi} d\varphi \int_0^\pi \sin \theta d\theta |\vec{n}\rangle \langle \vec{n}| = \mathbb{1}. \quad (44)$$

In light of this, it is possible to consider the expectation value of a generic $f(\hat{\theta}, \hat{\varphi})$ as

$$\langle l, m | f(\hat{\theta}, \hat{\varphi}) | l', m' \rangle = \int d\Omega \int d\Omega' \langle l, m | \vec{n} \rangle \langle \vec{n} | f(\hat{\theta}, \hat{\varphi}) | \vec{n}' \rangle \langle \vec{n}' | l', m' \rangle = \int d\Omega f(\theta, \varphi) \langle l, m | \vec{n} \rangle \langle \vec{n} | l', m' \rangle. \quad (45)$$

In the previous expression, one can recognize the emergence of the spherical harmonics [41], since $\langle \vec{n} | l', m' \rangle = Y_{l'}^{m'}(\theta, \varphi)$. Thus, the whole computation amounts to an evaluation of an integral over the solid angle of products of spherical harmonics. Indeed, the functions of the spherical angles in Eq. (43) can be written as linear superpositions of spherical harmonics with $l = 1$ as

$$\sin \theta \cos \varphi = \sqrt{\frac{2\pi}{3}} [Y_1^{-1}(\theta, \varphi) - Y_1^1(\theta, \varphi)], \quad \sin \theta \sin \varphi = i\sqrt{\frac{2\pi}{3}} [Y_1^{-1}(\theta, \varphi) + Y_1^1(\theta, \varphi)], \quad \cos \theta = \sqrt{\frac{4\pi}{3}} Y_1^0(\theta, \varphi). \quad (46)$$

With this knowledge, we can now solve the integrals by virtue of the formula [42]

$$\int d\Omega Y_{l_1}^{m_1}(\theta, \varphi) Y_{l_2}^{m_2}(\theta, \varphi) Y_{l_3}^{m_3}(\theta, \varphi) = \sqrt{\frac{(2l_1+1)(2l_2+1)(2l_3+1)}{4\pi}} \begin{pmatrix} l_1 & l_2 & l_3 \\ 0 & 0 & 0 \end{pmatrix} \begin{pmatrix} l_1 & l_2 & l_3 \\ m_1 & m_2 & m_3 \end{pmatrix}, \quad (47)$$

where we identify the Wigner 3-j symbol

$$\begin{pmatrix} l_1 & l_2 & l_3 \\ m_1 & m_2 & m_3 \end{pmatrix} = \frac{(-1)^{l_1-l_2-m_3}}{\sqrt{2l_3+1}} C_{l_1 m_1 l_2 m_2}^{l_3 -m_3}, \quad (48)$$

with C being the Clebsch-Gordan coefficients.

Finally, using the property $(Y_l^m(\theta, \varphi))^* = (-1)^m Y_l^{-m}(\theta, \varphi)$, we can cast the transition amplitude of the dipole moment \hat{d} in the following form:

$$\langle l, m | \hat{d} | l', m' \rangle = (-1)^m q_{\text{eff}} R \sqrt{(2l+1)(2l'+1)} \begin{pmatrix} 1 & l & l' \\ 0 & 0 & 0 \end{pmatrix} \left[\begin{pmatrix} 1 & l & l' \\ -1 & -m & m' \end{pmatrix} \frac{\vec{e}_x + i\vec{e}_y}{\sqrt{2}} + i \begin{pmatrix} 1 & l & l' \\ 1 & -m & m' \end{pmatrix} \frac{i\vec{e}_x + \vec{e}_y}{\sqrt{2}} + \begin{pmatrix} 1 & l & l' \\ 0 & -m & m' \end{pmatrix} \vec{e}_z \right]. \quad (49)$$

It is worth stressing that the assumption of an atom-like structure for the microspheres has led to the employment of a simple form for the dipole moments. However, to account for a more realistic scenario, the effective charge q_{eff} has to be properly estimated and must include all the effects that pertain to a mesoscopic body.

The Wigner 3-j symbols carry the following selection rules

1. $\begin{pmatrix} 1 & l & l' \\ 0 & 0 & 0 \end{pmatrix} \rightarrow |l-1| \leq l' \leq l+1,$
2. $\begin{pmatrix} 1 & l & l' \\ -1 & -m & m' \end{pmatrix} \rightarrow m' = m+1,$
3. $\begin{pmatrix} 1 & l & l' \\ 1 & -m & m' \end{pmatrix} \rightarrow m' = m-1,$

$$4. \begin{pmatrix} 1 & l & l' \\ 0 & -m & m' \end{pmatrix} \rightarrow m' = m.$$

Since Eq. (41) only requires the jump operators (31) for which $\Delta > 0$, we have

$$\hat{A}(\Delta > 0) = d_{\text{eff}} \sum_{\substack{m, m' \\ l, l' \text{ s.t. } E_{l'} - E_l = \frac{\hbar^2}{2I} \Delta}} M_{l, l', m} \begin{pmatrix} 1 & l & l' \\ 0 & 0 & 0 \end{pmatrix} \left[\begin{pmatrix} 1 & l & l' \\ -1 & -m & m' \end{pmatrix} \vec{v}_1 + i \begin{pmatrix} 1 & l & l' \\ 1 & -m & m' \end{pmatrix} \vec{v}_2 + \begin{pmatrix} 1 & l & l' \\ 0 & -m & m' \end{pmatrix} \vec{v}_3 \right] |l, m\rangle\langle l', m'|, \quad (50)$$

where $d_{\text{eff}} := q_{\text{eff}} R$, $M_{l, l', m} := (-1)^m \sqrt{(2l+1)(2l'+1)}$ and we define the rotated basis $\{\vec{v}_1 = (\vec{e}_x + i\vec{e}_y)/\sqrt{2}, \vec{v}_2 = (i\vec{e}_x + \vec{e}_y)/\sqrt{2}, \vec{v}_3 = \vec{e}_z\}$. The selection rule number (1), along with the fact that $E_{l'} - E_l > 0$ and that l, l' non-negative are integers imply that the only non-vanishing contributions to the sum are those with $l' = l + 1$. Since Δ is a fixed value, only the term with $l = \Delta/2 - 1$ contributes to the sum. Then, including the selection rules for m we have

$$\hat{A}_1(\Delta) = \sum_{m=-l}^l M_{l, l+1, m} \begin{pmatrix} 1 & l & l+1 \\ 0 & 0 & 0 \end{pmatrix} \begin{pmatrix} 1 & l & l+1 \\ -1 & -m & m+1 \end{pmatrix} |l, m\rangle\langle l+1, m+1| \quad (51)$$

$$\hat{A}_2(\Delta) = \sum_{m=-l}^l i M_{l, l+1, m} \begin{pmatrix} 1 & l & l+1 \\ 0 & 0 & 0 \end{pmatrix} \begin{pmatrix} 1 & l & l+1 \\ 1 & -m & m-1 \end{pmatrix} |l, m\rangle\langle l+1, m-1| \quad (52)$$

$$\hat{A}_3(\Delta) = \sum_{m=-l}^l M_{l, l+1, m} \begin{pmatrix} 1 & l & l+1 \\ 0 & 0 & 0 \end{pmatrix} \begin{pmatrix} 1 & l & l+1 \\ 0 & -m & m \end{pmatrix} |l, m\rangle\langle l+1, m| \quad (53)$$

where \hat{A}_k is the k -th component of vector (50) and for simplicity we have omitted that $l = l(\Delta)$.

Finally, since there is a one-to-one correspondence between l and Δ , we can change the summation index in Eq. (41) to write

$$\begin{aligned} \frac{d}{dt} \hat{\rho}_S(t) &= -\frac{i}{\hbar} [\hat{H}_I^{AB}, \hat{\rho}_S(t)] \\ &+ \sum_{l \geq 0} \frac{\Delta_l^3 \hbar^2}{6c^3 I^3 \epsilon_0} (1 + N(\Delta_l)) \left[\hat{A}^{AB}(\Delta_l) \cdot \hat{\rho}_S(t) \hat{A}^{AB\dagger}(\Delta_l) - \frac{1}{2} \left\{ \hat{A}^{AB\dagger}(\Delta_l) \cdot \hat{A}^{AB}(\Delta_l), \hat{\rho}_S(t) \right\} \right] \\ &+ \sum_{l \geq 0} \frac{\Delta_l^3 \hbar^2}{6c^3 I^3 \epsilon_0} N(\Delta_l) \left[\hat{A}^{AB\dagger}(\Delta_l) \cdot \hat{\rho}_S(t) \hat{A}^{AB}(\Delta_l) - \frac{1}{2} \left\{ \hat{A}^{AB}(\Delta_l) \cdot \hat{A}^{AB\dagger}(\Delta_l), \hat{\rho}_S(t) \right\} \right], \quad (54) \end{aligned}$$

where $\Delta_l := 2(l+1)$ and $\hat{A}^{AB} = \sum_i \hat{A}_i \vec{v}_i \otimes \mathbb{1} + \mathbb{1} \otimes \sum_i \hat{A}_i \vec{v}_i$ as given by Eqs. (51-53).

* trinidad.lantano-pinto@uni-ulm.de

† luciano.petruziello@uni-ulm.de

‡ susana.huelga@uni-ulm.de

§ martin.plenio@uni-ulm.de

- [1] C. M. Dewitt and D. Rickles, in *The role of gravitation in physics: report from the 1957 Chapel Hill Conference* (2011).
- [2] N. H. Lindner and A. Peres, Testing quantum superpositions of the gravitational field with Bose-Einstein condensates, *Physical Review A* **71**, 024101 (2005).
- [3] D. Kafri and J. M. Taylor, A noise inequality for classical forces, (2013), arXiv:1311.4558 [quant-ph].
- [4] J. Schmöle, M. Dragosits, H. Hepach, and M. Aspelmeyer, A micromechanical proof-of-principle experiment for measuring the gravitational force of milligram masses, *Classical and Quantum Gravity* **33**, 125031 (2016).
- [5] S. Bose, A. Mazumdar, G. W. Morley, H. Ulbricht, M. Toroš,

M. Paternostro, A. A. Geraci, P. F. Barker, M. S. Kim, and G. Milburn, Spin entanglement witness for quantum gravity, *Physical Review Letters* **119**, 240401 (2017).

- [6] A. Al Balushi, W. Cong, and R. B. Mann, Optomechanical quantum Cavendish experiment, *Phys. Rev. A* **98**, 043811 (2018).
- [7] T. Krisnanda, G. Y. Tham, M. Paternostro, and T. Paterek, Observable quantum entanglement due to gravity, *npj Quantum Information* **6**, 12 (2020).
- [8] H. Miao, D. Martynov, H. Yang, and A. Datta, Quantum correlations of light mediated by gravity, *Physical Review A* **101**, 063804 (2020).
- [9] H. Chevalier, A. J. Paige, and M. S. Kim, Witnessing the non-classical nature of gravity in the presence of unknown interactions, *Physical Review A* **102**, 022428 (2020).
- [10] J. S. Pedernales, G. W. Morley, and M. B. Plenio, Motional dynamical decoupling for interferometry with macroscopic particles, *Physical Review Letters* **125**, 023602 (2020).
- [11] A. Matsumura and K. Yamamoto, Gravity-induced entangle-

- ment in optomechanical systems, *Phys. Rev. D* **102**, 106021 (2020).
- [12] F. Cosco, J. S. Pedernales, and M. B. Plenio, Enhanced force sensitivity and entanglement in periodically driven optomechanics, *Physical Review A* **103**, L061501 (2021).
- [13] T. Weiss, M. Roda-Llorges, E. Torrontegui, M. Aspelmeyer, and O. Romero-Isart, Large quantum delocalization of a levitated nanoparticle using optimal control: Applications for force sensing and entangling via weak forces, *Physical Review Letters* **127**, 023601 (2021).
- [14] D. Miki, A. Matsumura, and K. Yamamoto, Entanglement and decoherence of massive particles due to gravity, *Phys. Rev. D* **103**, 026017 (2021).
- [15] J. S. Pedernales, K. Streltsov, and M. B. Plenio, Enhancing gravitational interaction between quantum systems by a massive mediator, *Physical Review Letters* **128**, 110401 (2022).
- [16] M. B. Plenio and S. Virmani, An introduction to entanglement measures, *Quantum Inf. Comput.* **7**, 1 (2007).
- [17] L. Lami, J. S. Pedernales, and M. B. Plenio, Testing the quantumness of gravity without entanglement, *Physical Review X* **14**, 021022 (2024).
- [18] D. Kafri, J. M. Taylor, and G. J. Milburn, A classical channel model for gravitational decoherence, *New Journal of Physics* **16**, 065020 (2014).
- [19] D. Kafri, G. J. Milburn, and J. M. Taylor, Bounds on quantum communication via Newtonian gravity, *New Journal of Physics* **17**, 015006 (2015).
- [20] J. S. Pedernales and M. B. Plenio, On the origin of force sensitivity in tests of quantum gravity with delocalised mechanical systems, *Contemp. Phys.* **64**, 147 (2023).
- [21] Y. Y. Fein, P. Geyer, P. Zwick, F. Kialka, S. Pedalino, M. Mayor, S. Gerlich, and M. Arndt, Quantum superposition of molecules beyond 25 kda, *Nature Physics* **15**, 1242 (2019).
- [22] R. M. Wald, Gravitational spin interaction, *Phys. Rev. D* **6**, 406 (1972).
- [23] C. W. Misner, K. S. Thorne, and J. A. Wheeler, *Gravitation* (W. H. Freeman, San Francisco, 1973).
- [24] S. Weinberg, *Gravitation and Cosmology: Principles and Applications of the General Theory of Relativity* (John Wiley and Sons, New York, 1972).
- [25] I. Güllü and B. Tekin, Massive Higher Derivative Gravity in D-dimensional Anti-de Sitter Spacetimes, *Phys. Rev. D* **80**, 064033 (2009).
- [26] I. Güllü and B. Tekin, Spin-Spin Interactions in Massive Gravity and Higher Derivative Gravity Theories, *Phys. Lett. B* **728**, 268 (2014).
- [27] J. F. Donoghue, General relativity as an effective field theory: The leading quantum corrections, *Phys. Rev. D* **50**, 3874 (1994).
- [28] J. F. Donoghue, Leading quantum correction to the Newtonian potential, *Phys. Rev. Lett.* **72**, 2996 (1994).
- [29] Y. Jin, J. Yan, S. J. Rahman, J. Li, X. Yu, and J. Zhang, 6 ghz hyperfast rotation of an optically levitated nanoparticle in vacuum, *Photon. Res.* **9**, 1344 (2021).
- [30] C. Wang, P. Bai, and X. Guo, Advances in separation methods for large-scale production of silicon isotopes, *Journal of Radioanalytical and Nuclear Chemistry* **304**, 989 (2015).
- [31] M. B. Plenio, Logarithmic Negativity: A Full Entanglement Monotone That is not Convex, *Phys. Rev. Lett.* **95**, 090503 (2005).
- [32] K. Walter, B. A. Stickler, and K. Hornberger, Collisional decoherence of polar molecules, *Phys. Rev. A* **93**, 063612 (2016).
- [33] B. Papendell, B. A. Stickler, and K. Hornberger, Quantum angular momentum diffusion of rigid bodies, *New Journal of Physics* **19**, 122001 (2017).
- [34] J. Bateman, S. Nimmrichter, K. Hornberger, and H. Ulbricht, Near-field interferometry of a free-falling nanoparticle from a point-like source, *Nature Commun.* **5**, 4788 (2014).
- [35] M. O. E. Steiner, J. S. Pedernales, and M. B. Plenio, Pentacene-Doped Naphthalene for Levitated Optomechanics, (2024), [arXiv:2405.13869 \[quant-ph\]](https://arxiv.org/abs/2405.13869).
- [36] P. Debye, Zur Theorie der spezifischen Wärmen, *Annalen Phys.* **344**, 789 (1912).
- [37] R. K. Iler, *The Chemistry of Silica* (Wiley & Sons Ltd., 1979).
- [38] G. Higgins, A. Di Biagio, and M. Christodoulou, Gravitationally Mediated Entanglement with Superpositions of Rotational Energies, (2024), [arXiv:2403.02062 \[quant-ph\]](https://arxiv.org/abs/2403.02062).
- [39] H.-P. Breuer and F. Petruccione, *The Theory of Open Quantum Systems* (Oxford University Press, 2007).
- [40] H. C. Fogedby, Field-theoretical approach to open quantum systems and the Lindblad equation, *Phys. Rev. A* **106**, 022205 (2022).
- [41] J. J. Sakurai and J. Napolitano, *Modern Quantum Mechanics*, Quantum physics, quantum information and quantum computation (Cambridge University Press, 2020).
- [42] I. S. Gradshteyn and I. M. Ryzhik, *Table of Integrals, Series, and Products* (1943).